

IUCrJ

Volume 2 (2015)

Supporting information for article:

Percolating Hierarchical Defect Structures drive Phase Transformation in Ce_{1-x}Gd_xO_{2-x/2}: a Total Scattering Study

Marco Scavini, Mauro Coduri, Mattia Allieta, Paolo Masala, Serena Cappelli, Cesare Oliva, Michela Brunelli, Francesco Orsini and Claudio Ferrero

Percolating hierarchical defect structures in

Ce_{1-x}Gd_xO_{2-x/2}: a total scattering study

Marco Scavini^{a,b}, Mauro Coduri^{a,c}, Mattia Allieta^a, Paolo Masala^a, Serena Cappelli^a, Cesare
Oliva^{a,b}, Michela Brunelli^d, Francesco Orsini^e, Claudio Ferrero^f

^aDipartimento di Chimica, Università di Milano, Via C. Golgi 19, I-20133 Milano, Italy

^bCNR-ISTM, Ist. Sci. & Tecnol. Mol., I-20133 Milan, Italy

^cIstituto per l'Energia e le Interfasi, CNR-IENI, C.so Promessi Sposi 29, 23900 Lecco, Italy

^dS.N.B.L./E.S.R.F., 71, Avenue des Martyrs, CS 40220, 38043 Grenoble Cedex 9,

France^eDipartimento di Fisica, Università di Milano, Via G. Celoria 19, I-20133 Milano, Italy

^fE.S.R.F.-The European Synchrotron, 71, Avenue des Martyrs, CS 40220, 38043 Grenoble Cedex 9,
France

Figure S1

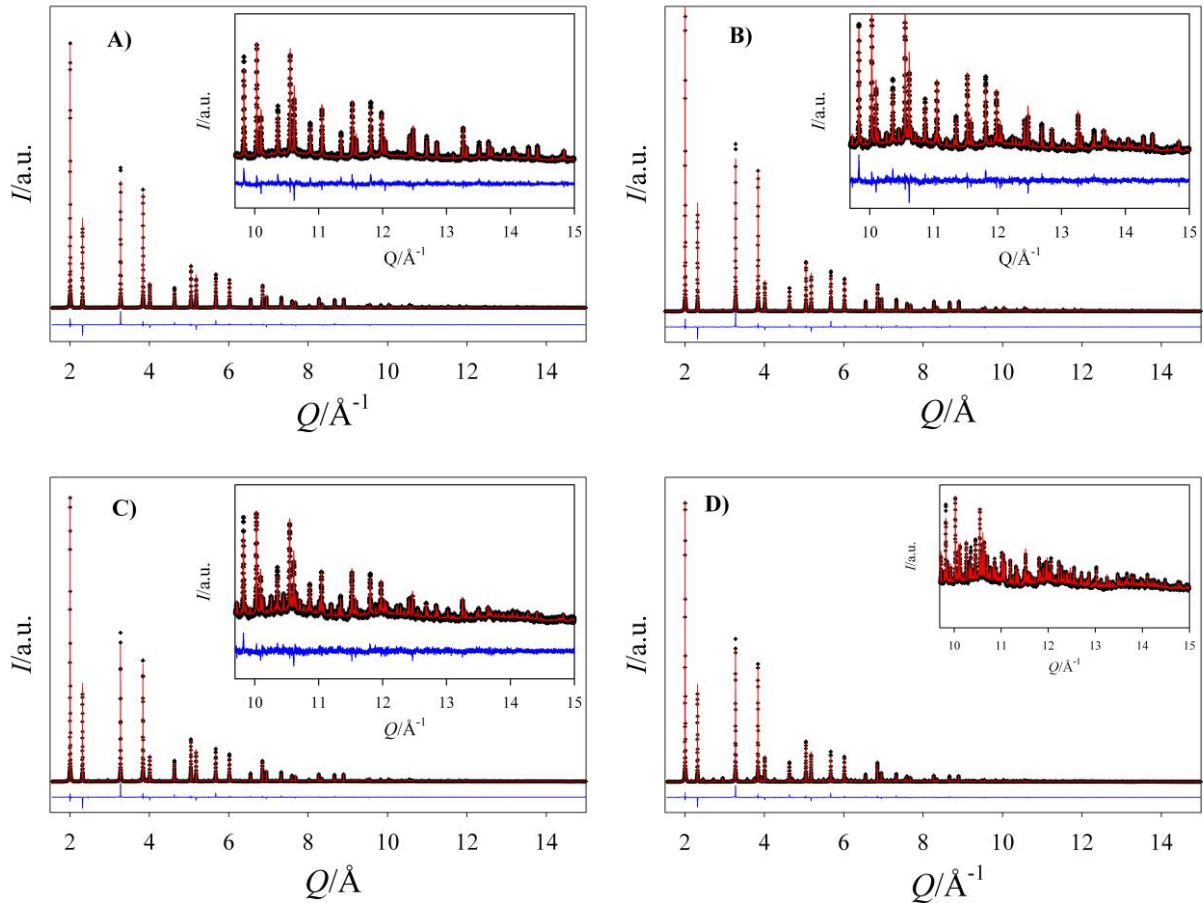


Figure S1 XRPD patterns of Ce_{1-x}Gd_xO_{2-x/2} samples and Rietveld refinements obtained using the structural models described in Table S1. A) $x_{\text{Gd}}=0.313$; B) $x_{\text{Gd}}=0.344$; C) $x_{\text{Gd}}=0.375$; D) $x_{\text{Gd}}=0.438$. Measured (black crosses) and calculated (red lines) profiles are shown as well as fit residuals (blue lines). The insets highlight the diffraction profiles in the high Q regions

Figure S2

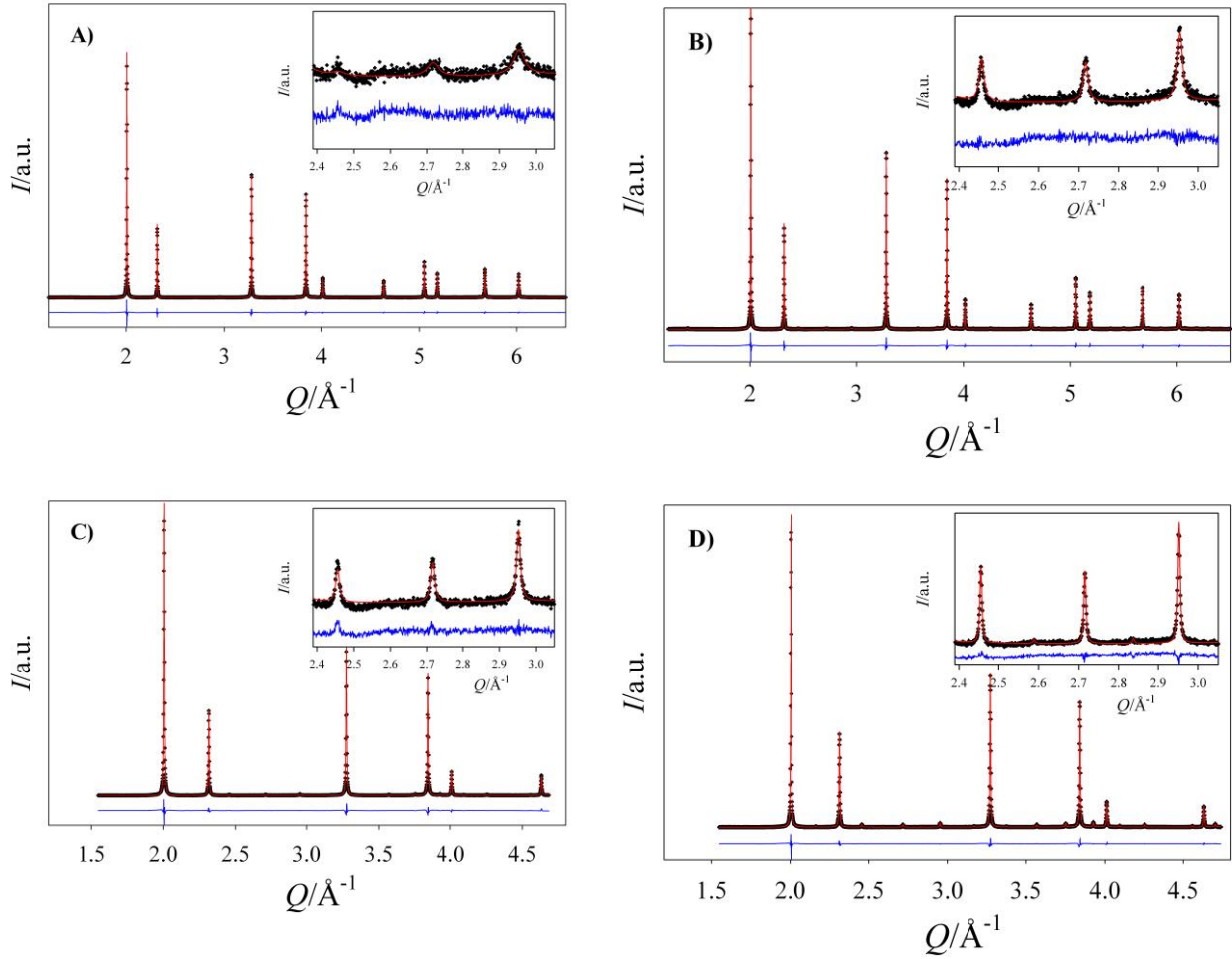


Figure S2 Same XRPD patterns as in Figure S1 using the WPPM approach. A) $x_{\text{Gd}}=0.313$; B) $x_{\text{Gd}}=0.344$; C) $x_{\text{Gd}}=0.375$; D) $x_{\text{Gd}}=0.438$. Measured (black crosses) and calculated (red lines) profiles are shown as well as fit residuals (blue lines). The insets highlight the diffraction profiles in the Q regions corresponding to the most intense superstructure peaks

Sites	C-type	Shifted C-type	C-type with shifted origin	$2\times2\times2$ Fluorite	$1\times1\times1$ Fluorite
M1	8b: $\frac{1}{4}, \frac{1}{4}, \frac{1}{4}$	$\frac{1}{4}, \frac{1}{4}, \frac{1}{4}$	$\frac{1}{4}, \frac{1}{4}, 0$	$\frac{1}{4}, \frac{1}{4}, 0$	4a: $\frac{1}{2}, \frac{1}{2}, 0$
M2	24d $x, 0, \frac{1}{4}$	$\Delta x(M2), 0, \frac{1}{4}$	$\Delta x(M2), 0, 0$	$0, 0, 0$	4a: $0, 0, 0$
O1	48e x, y, z	$3/8 + \Delta x(O1), 1/8 + \Delta y(O1), 3/8 + \Delta z(O1)$	$3/8 + \Delta x(O1), 1/8 + \Delta y(O1), 1/8 + \Delta z(O1)$	$3/8, 1/8, 1/8$	8c: $\frac{3}{4}, \frac{1}{4}, \frac{1}{4}$
O2	16c x, x, x	$3/8 + \Delta x(O2), 3/8 + \Delta x(O2), 3/8 + \Delta x(O2)$	$3/8 + \Delta x(O2), 3/8 + \Delta x(O2), 1/8 + \Delta x(O2)$	$3/8, 3/8, 1/8$	8c: $\frac{3}{4}, \frac{3}{4}, \frac{1}{4}$

Table S1. Scheme of the relationship between fluorite and C-type phases.

Column-wise legend: **C-type**: atom positions and corresponding Wyckoff symbols for the sites in the C-type structure; **Shifted C-type**: same setting as the previous column, with addition of the Δ values with respect to special positions; **C-type with shifted origin**: the cell origin is shifted with respect to the previous column by $<0, 0, \frac{1}{4}>$; **$2\times2\times2$ Fluorite**: same as the previous column with all Δ values set to zero to recover the fluorite structure; **$1\times1\times1$ Fluorite**: atom positions and corresponding Wyckoff symbols for the sites in the fluorite structure.

Sample	$x_{\text{Gd}}=0.313$	$x_{\text{Gd}}=0.344$	$x_{\text{Gd}}=0.375$	$x_{\text{Gd}}=0.438$
Space group	<i>Ia-3</i>	<i>Ia-3</i>	<i>Ia-3</i>	<i>Ia-3</i>
a/Å	10.84730(2)	10.84760(5)	10.85483(6)	10.85488(5)
$x_{\text{M}2}$	-0.00373(5)	-0.00548(5)	-0.00820(5)	-0.01309(3)
$x_{\text{O}1}$	3/8	3/8	0.376(1)	0.3778(5)
$y_{\text{O}1}$	1/8	1/8	0.135(1)	0.1412(5)
$z_{\text{O}1}$	3/8	3/8	0.378(2)	0.3774(8)
$x, y, z_{\text{O}2}$	3/8	3/8	0.377(4)	0.3775(2)
$U_{11}/U_{\text{iso}}(\text{M}1)$	0.012(1)	0.016(1)	0.0178(9)	0.02341(4)
$U_{12}(\text{M}1)$	-----	0.0105(8)	0.0058(9)	0.0122(4)
$U_{11}/U_{\text{iso}}(\text{M}2)$	0.0114(3)	0.0082(6)	0.0094(4)	0.0077(1)
$U_{22}(\text{M}2)$		0.016(1)	0.017(1)	0.0137(4)
$U_{33}(\text{M}2)$	-----	0.015(2)	0.016(1)	0.0150(5)
$U_{23}(\text{M}2)$	-----	-0.0069(6)	-0.0103(7)	-0.0116(2)
$U_{\text{iso}}(\text{O}1/\text{O}2)$	0.0191(3)	0.0215(4)	0.0209(6)	0.0184(6)
$R(F^2)$	0.0356	0.0485	0.0453	0.0609
R_P	0.0452	0.0479	0.0466	0.0418

Table S2. Rietveld refinement results referring to C-type $\text{Ce}_{1-x}\text{Gd}_x\text{O}_{2-x/2}$ samples with $x_{\text{Gd}}=0.313$, 0.344, 0.375 and 0.438. Fractional atomic coordinates are dimensionless, while the mean square displacements U_{iso} and U_{ij} are expressed in Å². The estimated standard deviations are in brackets.

Best fit of PDF data at short r range using the monophasic and the biphasic models

The PDF experimental profiles were best fitted using either the monophasic or the biphasic model (see Figure 4 in the text).

As to the *monophasic model*, the C-type structure was assumed (space group *Ia-3*) for all the samples in the C* zone, varying the cell constant, the $x(M2)$ coordinate and three different isotropic *msd* parameters for M1, M2 and O1/O2 positions. The refined parameters are reported in Table S2a.

As to the *biphasic model*, coexisting CeO₂ (*Fm-3m*) and Gd₂O₃ (*Ia-3*) were allowed for, keeping site occupations and O coordinates fixed to pure ceria and gadolinia values. In order to avoid over-parameterization and consequent parameter correlations, in the *biphasic model* only two cell parameters, the phase fractions, the $x(M2)$ coordinates, one *msd* parameter for all cationic sites and another *msd* parameter for all the anionic sites in the two phases were allowed to vary. The optimized parameters are reported in Table S2b.

Sample	$x_{\text{Gd}}=0.313$	$x_{\text{Gd}}=0.344$	$x_{\text{Gd}}=0.375$	$x_{\text{Gd}}=0.438$
Space group	<i>Ia-3</i>	<i>Ia-3</i>	<i>Ia-3</i>	<i>Ia-3</i>
a/Å	10.7248(8)	10.7064(7)	10.7002(8)	10.6492(5)
x_{M2}	-0.0003(2)	-0.0005(2)	-0.0063(2)	-0.0042(1)
$U_{\text{iso}}(\text{M1})$	0.0255(6)	0.02916(6)	0.0190(8)	0.0060(1)
$U_{\text{iso}}(\text{M2})$	0.00418(6)	0.00590(6)	0.0058(1)	0.00898(7)
$U_{\text{iso}}(\text{O})$	0.0558(8)	0.0578(6)	0.067(1)	0.022(1)
Rw	0.218	0.233	0.268	0.303

Table S2a. Real space Rietveld refinement (based on the monophasic model) of the calculated $G(r)$ curves in the $1.5 \leq r \leq 6.1$ Å range. The fractional atomic coordinates are dimensionless, while the *msd* U_{iso} are expressed in Å². The estimated standard deviations are in brackets.

Sample	$x_{\text{Gd}}=0.313$	$x_{\text{Gd}}=0.344$	$x_{\text{Gd}}=0.375$	$x_{\text{Gd}}=0.438$
Fluorite phase: space group $Fm\text{-}3m$				
a/Å	5.3729(6)	5.3638(4)	5.3593(5)	5.3450(3)
% .fluorite phase	68.2(3)	63.9(2)	61.9(3)	57.0(1)
C-type phase: space group $Ia\text{-}3$				
a/Å	11.060(3)	11.039(2)	11.047(3)	11.040 (1)
x_{M2}	-0.0275(2)	-0.0284(1)	-0.0293(2)	-0.03136(6)
% .C-type phase	31.8(3)	36.1(2)	38.1(3)	43.0(1)
Common parameters				
$U_{\text{iso}}(\text{M})$	0.00566(5)	0.00575(5)	0.00590(6)	0.00607(3)
$U_{\text{iso}}(\text{O})$	0.0534(8)	0.0487(8)	0.051(1)	0.0578(6)
Rw	0.096	0.091	0.097	0.118

Table S2b. Real space Rietveld refinement (based on the biphasic model) of the calculated $G(r)$ curves in the $1.5 \leq r \leq 6.1$ Å range. The fractional atomic coordinates are dimensionless, while the *msd* U_{iso} are expressed in Å². The estimated standard deviations are in brackets